



# Evolution of the Accretion Rate of Young Intermediate-mass Stars: Implications for Disk Evolution and Planet Formation

Sean D. Brittain<sup>1</sup> , Joshua W. Kern<sup>1</sup> , Gwendolyn Meeus<sup>2</sup> , and René D. Oudmaijer<sup>3,4</sup>

<sup>1</sup> Department of Physics and Astronomy, Clemson University, Clemson, SC 29634-0978, USA

<sup>2</sup> Universidad Autonoma de Madrid, Madrid, Spain

<sup>3</sup> Royal Observatory of Belgium, Ringlaan 3, 1180 Brussels, Belgium

<sup>4</sup> School of Physics and Astronomy, University of Leeds, Leeds LS2 9JT, UK

Received 2025 May 27; revised 2025 October 24; accepted 2025 October 24; published 2025 December 3

## Abstract

This work presents a study of the evolution of the stellar accretion rates of pre-main-sequence intermediate-mass stars. We compare the accretion rate of the younger intermediate-mass T Tauri stars (IMTTSs) with the older Herbig stars into which they evolve. We find that the median accretion rate of IMTTSs ( $1.2 \times 10^{-8} M_{\odot} \text{ yr}^{-1}$ ) is significantly lower than that of Herbig stars ( $1.9 \times 10^{-7} M_{\odot} \text{ yr}^{-1}$ ). This increase stands in stark contrast with canonical models of disk evolution that predict that the stellar accretion rate declines with age. We put forward a physically plausible scenario that accounts for the systematic increase of stellar accretion based on the increase of the effective temperature of the stars as they evolve towards the zero-age main sequence. For example, the temperature of a  $2M_{\odot}$  star will increase from 4900 K in the IMTTS phase to 9100 K during the Herbig phase. Thus, the luminosity of the far-ultraviolet (FUV) radiation will increase by orders of magnitude. We propose that this increase drives a higher stellar accretion rate. The scenario we propose to account for the increase in the stellar accretion rate solves the lifetime problem for Herbig disks because the increasing stellar accretion rates require lower initial disk masses to account for present-day disk masses. This work highlights the importance of the role FUV radiation has in driving the accretion rate, predicts a large population of pre-main-sequence nonaccreting A stars, and has implications for interpreting disk morphologies that may serve as signposts of embedded gas giant planets in Herbig disks.

*Unified Astronomy Thesaurus concepts:* [Stellar accretion disks \(1579\)](#); [Protoplanetary disks \(1300\)](#); [Circumstellar disks \(235\)](#); [Herbig Ae/Be stars \(723\)](#); [T Tauri stars \(1681\)](#); [Intermediate-type stars \(818\)](#)

## 1. Introduction

Herbig stars are pre-main-sequence stars that represent an interesting transition between low-mass stars and high-mass stars (see I. Mendigutía 2020; S. D. Brittain et al. 2023 for recent reviews). Like their lower mass counterparts, the classical T Tauri stars (CTTSs), they reveal extended disks with structures indicative of ongoing gas giant planet formation (R. Dong et al. 2018; M. Janson et al. 2021; L. M. Stapper et al. 2022). Magnetohydrodynamic (MHD) simulations of ionized disks have shown that the dynamics of the in situ disk gas are strongly affected by magnetic fields that thread the disk (X.-N. Bai 2011; X.-N. Bai & J. M. Stone 2013). In the inner disk, these magnetic fields largely arise from the star at the center of the disk. The energy transport mechanisms of T Tauri stars facilitate convection currents that drive strong, well-ordered magnetic fields on the order of a kilogauss (e.g., C. M. Johns-Krull 2007). In contrast, the higher temperatures of Herbig stars sufficiently ionize the outer layers, allowing for a purely radiative transfer of energy (F. Villebrun et al. 2019).

Although Herbig stars lack convection currents, magnetic fields have been measured in roughly 10% of Herbig stars in the range of  $\sim 100$ – $1000$  G (E. Alecian et al. 2013). These fields are likely fossil fields left over from a previous evolutionary phase as an intermediate-mass T Tauri star

(IMTTS) or the collapsing parent molecular cloud (M. Vioque et al. 2018).

Due to the dearth of strong, well-ordered stellar magnetic fields among Herbig stars, it was not expected that the magnetospheric accretion paradigm, so successful at characterizing accretion onto CTTSs, would apply to these earlier-type stars. However, several lines of evidence have emerged to the contrary. For example,  $H\alpha$  spectropolarimetric observations indicate that the star/disk interface of CTTSs and Herbig Ae stars is similar and consistent with the presence of an inner hole as expected from magnetically mediated accretion (J. S. Vink et al. 2002, 2005a, 2005b). An additional line of evidence comes from successfully modeling the hydrogen emission line profiles and the Balmer discontinuity of UX Ori using a magnetospheric model (J. Muzerolle et al. 2004). A third line of evidence comes from the observation of high-velocity redshifted absorption features superimposed on hydrogen emission lines that are indicative of gas in freefall onto these stars (M. M. Guimarães et al. 2006). An early effort to calibrate the line luminosity of  $\text{Br}\gamma$  to the accretion luminosity of Herbig stars as measured from the Balmer discontinuity found that the calibration was consistent with the relationship found for CTTSs (B. Donehew & S. Brittain 2011). Subsequent work applied to a larger sample and more lines found that these relationships extended to Herbig stars as early as B7 (I. Mendigutía et al. 2011; J. R. Fairlamb et al. 2017; C. Wichittanakom et al. 2020).

The relationship between the stellar mass and stellar accretion rate among CTTSs is also found for Herbig stars. C. Wichittanakom et al. (2020) found that this relationship



Original content from this work may be used under the terms of the [Creative Commons Attribution 4.0 licence](#). Any further distribution of this work must maintain attribution to the author(s) and the title of the work, journal citation and DOI.

extends to  $\sim 4M_{\odot}$  while the relationship is not as steep for the higher mass stars. Expanding on this, S. L. Grant et al. (2022) performed the largest high-resolution spectroscopic survey of Br $\gamma$  emission from Herbig stars, and confirmed these trends with the same break in the dependence of accretion rate on stellar mass occurring near  $M_{\star} \sim 4M_{\odot}$ . These studies largely confirm evidence from H $\alpha$  spectropolarimetry indicating that the star/disk interface changes for stars with masses  $\gtrsim 4M_{\odot}$  (J. S. Vink et al. 2002, 2005a, 2005b; J. S. Vink 2015; K. M. Ababakr et al. 2016, 2017).

Large surveys of the accretion rates of Herbig stars indicate that the median accretion rate of sources with  $M_{\star} \leq 4M_{\odot}$  is  $\sim 1.9 \times 10^{-7} M_{\odot} \text{ yr}^{-1}$  (J. R. Fairlamb et al. 2015, 2017; C. Wichittanakom et al. 2020). This is markedly higher than the median accretion rate of CTTSs in Taurus, which is  $1.3 \times 10^{-8} M_{\odot} \text{ yr}^{-1}$  (J. R. Najita et al. 2015).

C. Wichittanakom et al. (2020) noted that the relationship of stellar accretion rates with mass is also confounded with the age of the star. To explore the dependency of the stellar accretion rate on the age of the star, these authors selected a narrow range of stellar masses ( $2.0\text{--}2.5 M_{\odot}$ ) to minimize the mass dependency of the stellar accretion rate and determined that the accretion rate declines as  $\text{Age}^{-1.95 \pm 0.49}$ . If stellar accretion rates decline over time, which is expected for viscous accretion models with a constant  $\alpha$  (L. Hartmann et al. 1998), then we should expect the evolutionary precursors of Herbig stars (i.e., the IMTTs) to have accretion rates that are systematically higher than those of Herbig stars.

There are few studies dedicated to the study of IMTTs. These can be defined as stars with  $1.5 M_{\odot} \leq M_{\star} \leq 4.0 M_{\odot}$  and  $T_{\text{eff}} < 7,200 \text{ K}$  (i.e., stars with a spectral type of F0 or later). One important exception is a study of the accretion rate of nine IMTTs (N. Calvet et al. 2004). The average stellar accretion rate of these sources was found to be comparable to their lower-mass counterparts, the T Tauri stars with  $M_{\star} \leq 1.5 M_{\odot}$  ( $\dot{M} = 2.8 \times 10^{-8} M_{\odot} \text{ yr}^{-1}$ ). More recently, P. G. Viegand et al. (2021) determined the stellar parameters of a large sample of IMTTs (with mass limits  $1.5 M_{\odot} < M_{\star} < 3.5 M_{\odot}$ ) within 500 pc, which presents a new opportunity to expand the accretion statistics of this subclass of stars.

Here we extend the work of N. Calvet et al. (2004) by determining the accretion rate of an additional 33 IMTTs. We show that the accretion rates of IMTTs from the earlier study are representative of a much larger sample and about 1 order of magnitude less than the accretion rates of Herbig stars. We propose a solution for this counterintuitive result and discuss how it may account for the apparent discrepancy between the high accretion rate and relatively low disk mass of Herbig stars.

## 2. Sample

The sample of IMTTs included in this study was drawn from P. G. Viegand et al. (2021), for which a uniform set of stellar parameters had been determined. To restrict our sample to stars with spectral type F0 and later, we selected the stars with  $T_{\text{eff}} < 7200 \text{ K}$  for a total of 47 stars. We found the requisite data in the literature to calculate the stellar accretion rate for 42 of the stars in this sample (Table 1). To keep the calculation as uniform as possible, the accretion rate was determined from the luminosity of H $\alpha$  for 38 sources. There are four sources for which we did not find a measurement of H $\alpha$  in the literature, and we used alternative methods to

determine the stellar accretion rate. The accretion luminosities of two of these were adopted from values measured from the UV excess. One source was inferred from the luminosity of Pa $\beta$ , and the other source was inferred from the Br $\gamma$  luminosity. These are noted in Table 1. To convert the equivalent width H $\alpha$  to an accretion rate, we first inferred the intrinsic equivalent width of the line by correcting for photospheric absorption using model stellar atmospheres from P. R. T. Coelho (2014). We do not attempt to correct for the veiling of the H $\alpha$  photospheric line. Doing so would lower the accretion rates we infer and increase the disparity between the accretion rate of IMTTs and Herbig stars. The line flux was scaled using Gaia DR2 photometry to remain consistent with P. G. Viegand et al. (2021). We corrected for reddening based on the color excess reported by P. G. Viegand et al. (2021),  $R_V = 3.1$ , and the reddening law from J. A. Cardelli et al. (1989). The accretion luminosity was inferred from the luminosity of the H $\alpha$  line using the relationship determined by J. M. Alcalá et al. (2017). We adopted this relationship, calibrated against T Tauri stars rather than the relationship calibrated against Herbig stars by J. R. Fairlamb et al. (2017), because we expect the accretion geometry and magnetic field strengths of IMTTs to be more similar to CTTSs than to the radiative Herbig stars (F. Villebrun et al. 2019). The stellar accretion rate is proportional to the accretion luminosity so that

$$\dot{M} = \frac{L_{\text{acc}} R_{\star}}{GM_{\star}}, \quad (1)$$

where stellar parameters were taken from P. G. Viegand et al. (2021). The median of the stellar accretion rate of our IMTT sample is  $1.2 \times 10^{-8} M_{\odot} \text{ yr}^{-1}$ .

## 3. Accretion Rates

Herbig stars from J. R. Fairlamb et al. (2017, 2015), M. Vioque et al. (2018), and C. Wichittanakom et al. (2020) were chosen to compare their accretion rates with IMTTs. The Herbig star sample was limited to sources with  $7200 \text{ K} \leq T_{\text{eff}} \leq 13,000 \text{ K}$  and  $\log(L_{\star}) \leq 2.7 L_{\odot}$  to select stars with  $M_{\star} \lesssim 4M_{\odot}$  resulting in 89 stars. A histogram of the stellar accretion rates of IMTTs and Herbig stars is presented in Figure 1. The median accretion rate of Herbig stars is  $1.9 \times 10^{-7} M_{\odot} \text{ yr}^{-1}$ , which is over 1 order of magnitude higher than the median accretion rate of the IMTTs ( $1.2 \times 10^{-8} M_{\odot} \text{ yr}^{-1}$ ). Even if we decrease the log luminosity limit to  $2.3 L_{\odot}$  to restrict our sample to stars  $\lesssim 3.5 M_{\odot}$ , the median rate of Herbig stars is  $1.6 \times 10^{-7} M_{\odot} \text{ yr}^{-1}$ , which is still more than 1 order of magnitude higher than the median rates of IMTTs. The range of the log of accretion rates for the IMTTs spans from roughly  $-10$  to  $-6$ , while the range seen in Herbig stars spans from roughly  $-8$  to  $-4$ . Although sensitivity limits may restrict the identification of Herbig stars accreting at rates less than  $10^{-8} M_{\odot} \text{ yr}^{-1}$ , there is no evidence of a clustering of Herbig stars at this limit. IMTTs with accretion rates greater than  $10^{-7} M_{\odot} \text{ yr}^{-1}$  in the volume we consider are unlikely to be missed. In the Appendix, we address potential concerns about the reliability of measurements of the stellar accretion rate of Herbig stars and conclude that the inferred accretion rates of Herbig stars published in the literature are reliable.

To disentangle the dependency of the stellar accretion rate on stellar mass and age, we plot the mass accretion rates of

**Table 1**  
IMTTS Sample

Name	Teff (K)	$L_*/L_\odot$	$R$ Dereddened	$W_{H\alpha}$ (Å)	$\log(F_{H\alpha})$ (erg s <sup>-1</sup> cm <sup>-2</sup> )	$\log(L_{\text{Acc}})$ ( $L_\odot$ )	$\log(\dot{M})$ ( $M_\odot \text{ yr}^{-1}$ )	References
AK Sco	6250	6.94	8.6	-4.7	-11.1	-0.92	-8.2	(1)
Ass ChaT2-21 (a)	5660	10.37	8.3	-0.1	-13.1	-2.92	-10.2	(2)
Ass ChaT2-54 (b)	5260	5.03	9.4	...	...	-2.08	-9.4	(3)
BE Ori (a)	5720	7.95	10.2	-33.7	-11.3	-0.13	-7.4	(4)
Brun 252 (c)	5890	7.16	10.4	-4.0	-12.3	-1.22	-8.5	(5)
Brun 555	5040	11.37	10.3	-3.5	-12.3	-1.09	-8.3	(6)
Brun 656 (d)	5770	27.4	9.3	...	...	...	...	...
BX Ari (d)	5040	48.81	2.4	...	...	...	...	...
CO Ori	6030	43.82	10.1	-7.6	-11.9	-0.74	-7.9	(7)
CR Cha	4800	3.72	9.6	-30.8	-11.1	-0.58	-7.8	(7)
CV Cha	5280	4.63	9.4	-72.6	-10.6	-0.05	-7.4	(7)
DI Cep (e)	5490	9.82	9.4	...	...	0.18	-7.1	(8)
DI Cha	5770	9.82	8.5	-19.4	-10.9	-0.32	-7.6	(7)
EM*SR 21 (f)	5950	7.03	10.7	...	...	-1.92	<-9.2	(9)
EZ Ori	5830	7.54	10.5	-14.6	-11.8	-0.62	-7.9	(7)
GW Ori	5700	35.47	8.6	-31.8	-10.7	0.60	-6.6	(7)
GX Ori (b)	5410	3.1	11.8	...	...	-0.08	-7.5	(10)
Haro 1-6	5880	12.78	10.3	-4.5	-12.2	-2.17	-9.4	(11)
HBC 338	5490	5.67	9.9	-28.1	-11.3	-0.33	-7.7	(12)
HBC 415	5770	7.48	8.5	-7.3	-11.3	-0.93	-8.2	(6)
HBC 442	6170	13.2	9.7	-7.3	-11.8	-0.63	-7.9	(1)
HBC 502	4830	10.71	10.3	-4.5	-12.2	-1.08	-8.2	(13)
HD 135344B	6640	8.09	8.0	-9.7	-10.8	-0.52	-7.3	(1)
HD 142527	6500	19.31	7.4	-13.1	-10.3	0.65	-6.6	(1)
HD 288313A (d)	5040	38.47	9.0	...	...	...	...	...
HD 294260	6115	8.74	10.2	-16.5	-11.6	-0.40	-7.7	(7)
HD 34700	6060	24.34	8.8	...	-11.3	0.40	-6.8	(1)
HD 35929	7000	80.78	8.0	...	-10.9	0.91	-7.3	(1)
HQ Tau	5280	4.63	10.1	-4.1	-12.2	-1.98	-9.3	(14)
HT Lup	4830	5.95	8.7	-6.3	-11.4	-1.13	-8.3	(15)
LkH $\alpha$ 310	5590	6.8	12.8	-19.4	-12.6	-1.47	-8.8	(13)
LkH $\alpha$ 330	6240	14.39	9.2	...	-11.0	0.07	-7.2	(16)
PDS 115	5770	4.27	10.2	-11.8	-11.8	-0.93	-8.3	(15)
PDS 156	5660	21.12	8.2	-9.6	-11.0	0.22	-7.0	(15)
PDS 277	6720	9.68	9.8	...	-11.5	-0.47	-7.2	(1)
PR Ori (d)	5170	10.83	10.1	...	...	...	...	...
RY Ori	6120	9.01	10.0	...	-11.4	-0.24	-7.5	(1)
RY Tau	5945	11.97	8.8	-23.2	-10.9	-0.68	-7.1	(6)
SU Aur	5680	12.75	8.4	-6.6	-11.3	-0.95	-8.2	(6)
SW Ori	5490	3.28	11.2	-6.7	-12.4	-1.36	-9.0	(6)
T Tau	5700	8.88	8.0	-74.4	-10.1	0.30	-7.3	(7)
UX Tau A	5490	8.91	11.1	-8.5	-12.3	-2.19	-8.9	(7)
V1044 Ori	5500	6.1	10.6	-6.3	-12.2	-1.08	-7.7	(7)
V1650 Ori	6160	9.53	9.9	-14.2	-11.5	-0.50	-8.3	(17)
V2149 Ori (d)	6180	35.8	8.8	...	...	...	...	...
V395 Cep	5470	4.71	9.2	-10.2	-11.4	-0.95	-8.8	(6)
V815 Ori	5530	5.46	10.8	-5.2	-12.3	-1.24	-8.7	(6)

**Note.** The stellar temperature and luminosity are taken from P. G. Vælgård et al. (2021). The accretion luminosity is inferred from published values of the  $H\alpha$  unless otherwise noted. Notes: (a) The reported equivalent width was corrected for photospheric absorption. (b) The flux of  $H\alpha$  was not reported in the literature, so the  $L_{\text{acc}}$  inferred from the UV was used to calculate the accretion rate. (c) The equivalent width of  $H\alpha$  was extracted from the spectrum available in VizieR. (d) No data were found in the literature. (e) The accretion luminosity was inferred from a published value for Br $\gamma$ . (f) The accretion luminosity was inferred from a published value of Pa $\beta$ . References: (1) C. Wichittanakom et al. (2020); (2) F. M. Walter (1992); (3) C. F. Manara et al. (2017); (4) M. Fang et al. (2013); (5) F. Villebrun et al. (2019); (6) G. H. Herbig & K. R. Bell (1988); (7) B. Reipurth et al. (1996); (8) J. A. Eisner et al. (2007); (9) A. Natta et al. (2006); (10) N. Calvet et al. (2004); (11) E. L. N. Jensen et al. (2009); (12) G. Maheswar et al. (2003); (13) K. M. Flaherty & J. Muzerolle (2008); (14) M. N. Simon et al. (2016); (15) J. Gregorio-Hetem & A. Hetem (2002); (16) C. F. Manara et al. (2014); (17) G. Rojas et al. (2008).

these IMTTSs and Herbig stars on a Hertzsprung–Russell (H-R) diagram (Figure 2) with isochrones and evolutionary tracks from L. Siess et al. (2000). While there is some inconsistency among the more modern stellar models, the Siess models appear to be the most accurate at the higher mass end of pre-main-sequence stars (T. A. M. Braun et al. 2021). A

cursory examination of Figure 2 immediately reveals that the accretion rates of IMTTSs are systematically lower than those of Herbig stars. Tracing the zero-age main sequence (ZAMS), there is a clear trend between the stellar accretion rate and mass/age as noted previously by C. Wichittanakom et al. (2020). However, if one follows a given mass track (e.g.,

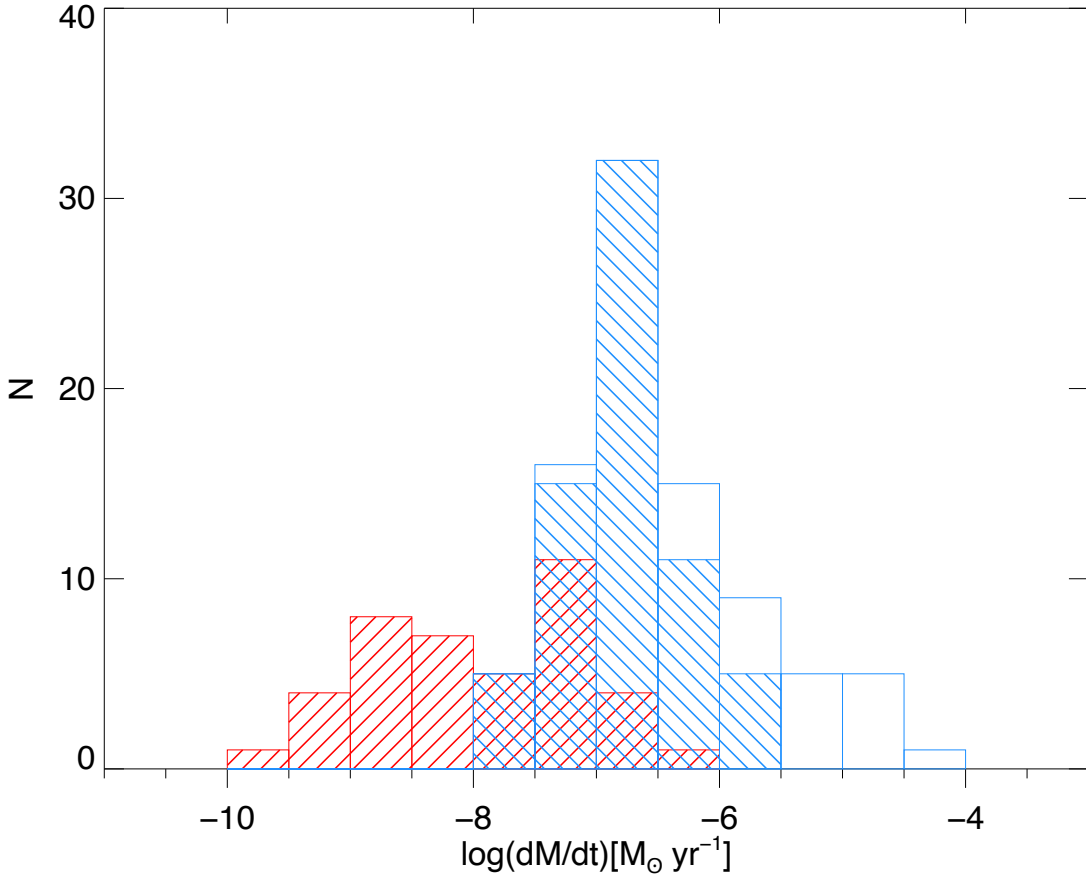


**Figure 1.** Distribution of the stellar accretion rates of all Herbig stars (blue) and IMTTs (red). The empty bins are Herbig stars with  $2.3 \lesssim \log(L_*/L_\odot) \lesssim 2.7$ . The median stellar accretion rate of Herbig stars is 1 order of magnitude higher than the median stellar accretion rate of IMTTs.

$M_* = 2M_\odot$ ), one can see the stellar accretion rate increase from  $10^{-9} M_\odot \text{ yr}^{-1}$  at about 1–3 Myr to  $10^{-7} M_\odot \text{ yr}^{-1}$  near the ZAMS.

An increase in the stellar accretion rate with age stands in stark contrast with what is predicted by viscous evolution models with a uniform  $\alpha$ , where the stellar accretion rate is expected to decline with age (L. Hartmann et al. 1998). The observed accretion rates of T Tauri stars in different clusters are consistent with such a model (e.g., J. Muzerolle et al. 2004; A. Sicilia-Aguilar et al. 2006). This suggests that the relationship between age and accretion rate for intermediate-mass objects is fundamentally different than that of their lower-mass counterparts.

#### 4. Modeling Accretion Evolution of Intermediate-mass Stars

The relatively high accretion rates of Herbig stars point to a well-known incongruity with the expected mass of the disk (e.g., I. Mendigutía et al. 2012; R. Dong et al. 2018; S. L. Grant et al. 2023). Indeed, the stellar accretion rate of Herbig stars scales weakly with the disk mass inferred from millimeter continuum observations,

$$\log(\dot{M}) = (-0.03 \pm 0.21)\log(M_{\text{disk}}) + (-6.99 \pm 0.52) \quad (2)$$

for  $-4.8 \lesssim \log(M_{\text{disk}}/M_\odot) \lesssim -1.2$  (S. L. Grant et al. 2023). The typical Herbig star is a few million years old with a stellar accretion rate of a few  $\times 10^{-7} M_\odot \text{ yr}^{-1}$ . Estimates of the disk mass inferred from millimeter measurements imply that the

lifetime of disks is only about 10% of the stellar age, assuming the observed stellar accretion rate is constant (I. Mendigutía et al. 2012; R. Dong et al. 2018). If the accretion rate declines as a power law with  $\dot{M}(t) \propto t^{-3/2}$ , as expected for viscous accretion with a uniform  $\alpha$  (L. Hartmann et al. 1998), then the minimum mass in the disk can be determined from integrating this expression such that

$$M_{\text{disk}}(t) = 2t\dot{M}(t). \quad (3)$$

As seen in Figure 2, the typical age and stellar accretion rate of a Herbig disk are a few Myr and  $10^{-7} M_\odot \text{ yr}^{-1}$ , respectively. If Equation (3) accurately approximates the time evolution of the stellar accretion rate, then the typical disk mass is  $\sim 30\%$  of the Herbig star mass. In this case, the disk mass inferred from millimeter measurements is underestimated by about 1 order of magnitude, and the typical Herbig disk is gravitationally unstable. Furthermore, the stellar accretion rates would imply implausibly high disk masses during the IMTTs phase.

Here, we explore a scenario that can account for the increase in the stellar accretion rate as the star evolves toward the main sequence and resolves the apparent incongruity between the inferred stellar accretion rate and disk mass of Herbig stars. Unlike their lower-mass counterparts, intermediate-mass stars spend a substantial fraction of their pre-main-sequence evolution along the radiative Henyey tracks. Thus, the temperature of intermediate-mass stars will increase by a factor of 2 or more as they evolve to the ZAMS (Figure 2). As a result, the luminosity of the far-ultraviolet (FUV) continuum

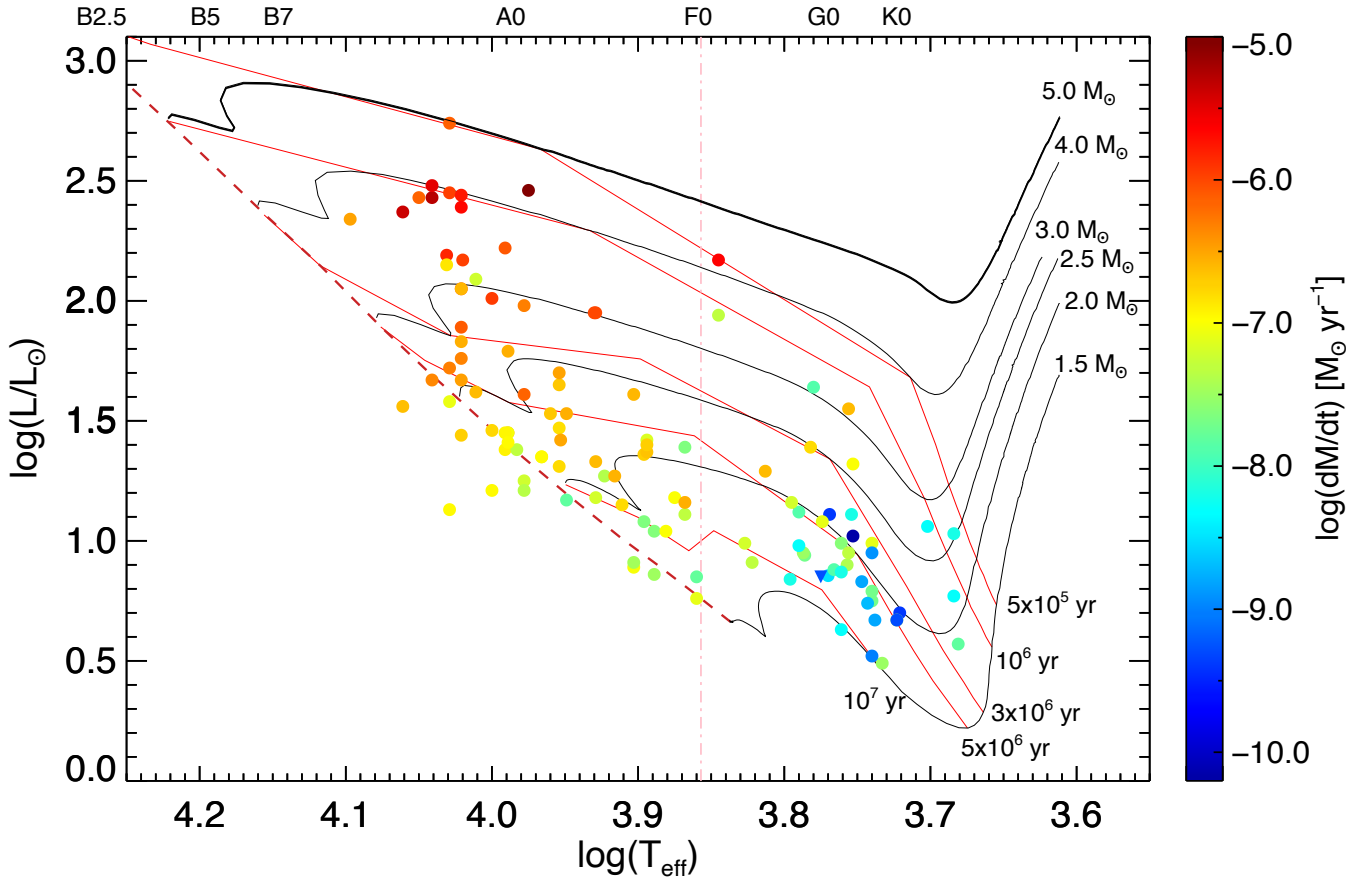


**Figure 2.** Mass accretion rate of IMTTs and Herbig stars. The stellar mass accretion rate is indicated by the color. The evolutionary tracks and isochrones are from the Siess stellar evolution model (L. Siess et al. 2000). The stellar luminosity and temperature were adopted from P. G. Valsegard et al. (2021), J. R. Fairlamb et al. (2015), M. Vioque et al. (2018), and C. Wichittanakom et al. (2020). The early main sequence is indicated by the red dashed line. The brown dashed line demarcates Herbig stars and IMTTs.

( $\sim 6\text{--}13.6\text{ eV}$ ) can increase by as much as 4 orders of magnitude.

M. Kunitomo et al. (2021) explored the role of stellar evolution on the photoevaporation of disks around intermediate-mass stars. These authors found that the sharp increase in the FUV luminosity of these stars accelerated the dispersal of the disks. However, the FUV irradiation of disks can also affect how the disks accrete.

In MHD simulations of wind-driven accretion, the accretion rate depends strongly on the penetration depth of the FUV field and the surface density of the FUV ionized layer in the disk atmosphere (X.-N. Bai & J. M. Stone 2013). Similar conclusions have been found in MHD simulations of accretion flows driven by in-disk angular momentum transport due to the magnetorotational instability (MRI). X.-N. Bai (2011) argued that the total MRI-driven accretion rate in the inner disk is significantly affected by the FUV ionization, and the FUV could even be the main source of ionization in the outer disk. The effects of FUV ionization on surface layer accretion were modeled by D. Perez-Becker & E. Chiang (2011), in which the surface density of the MRI active layer scales as  $\Sigma_* \propto L_{\text{FUV}}^{1/2}$ .

If disks accrete through their surface, and if that accretion (whether driven by disk winds or another in-disk angular momentum transport mechanism) is proportional to the surface density of the ionized layer, then one would expect that the accretion rate would increase as the stellar radiation field hardens. Regardless of the details of how accretion and other mechanisms of disk dispersal (e.g., photoevaporation) affect

the disk as the gas is depleted and becomes optically thin, when this occurs, accretion in these systems effectively stops.

To illustrate the effect of stellar evolution on the accretion rate of an intermediate-mass star, we consider a toy model in which the stellar accretion rate initially declines as  $t^{-3/2}$  as one might expect for viscous accretion with a constant  $\alpha$  (see, for example, L. Hartmann et al. 1998). We add a component to the accretion rate that scales as  $L_{\text{FUV}}^{1/2}$  (D. Perez-Becker & E. Chiang 2011). Thus, the time dependence of the stellar accretion rate is described by

$$\dot{M}(t) = 10^{-9} M_{\odot} \text{ yr}^{-1} \left( \frac{t}{0.5 \text{ Myr}} \right)^{-3/2} + 2 \times 10^{-7} M_{\odot} \text{ yr}^{-1} \left( \frac{L_{\text{FUV}}(t)}{L_{\odot}} \right)^{1/2}. \quad (4)$$

We consider a  $2M_{\odot}$  star with a disk that begins just marginally gravitationally unstable ( $M_{\text{disk}} = 0.15M_*$ ) at 0.5 Myr (see, for example, C. Hall et al. 2019). The fiducial stellar accretion rates in Equation (4) were chosen to reflect the typical beginning and ending accretion rates of  $2M_{\odot}$  stars in our sample. To determine the FUV luminosity, we assume that the FUV is dominated by the continuum emission of the stellar photosphere. While several lines in the FUV scale with the accretion luminosity (N. Calvet et al. 2004), the integrated luminosity of these lines is 1–3 orders of magnitude lower than the continuum luminosity at the stellar accretion rates covered by our sample. We integrate the flux from the stellar models



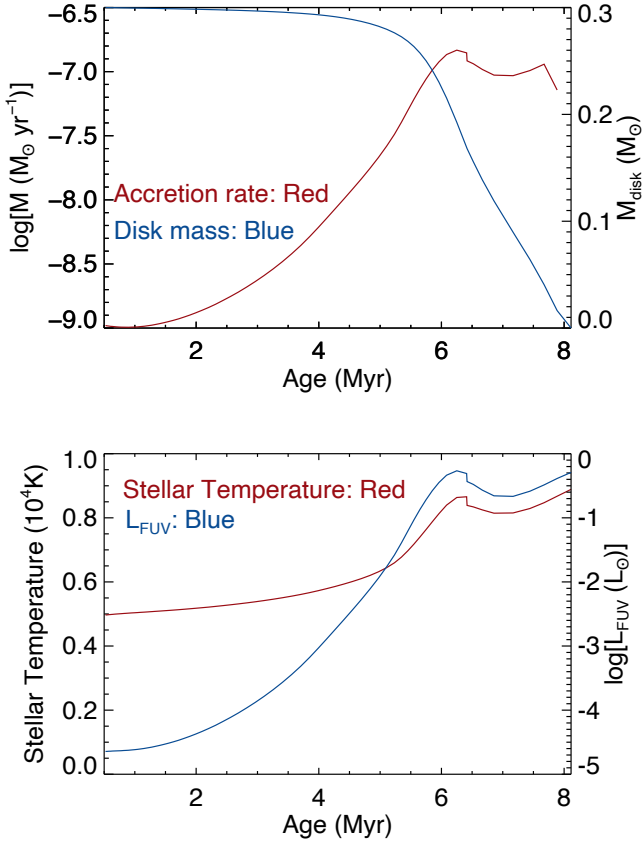


**Figure 3.** Comparison of the accretion rate (red) and disk mass (blue) in the upper panel and the effective temperature (red) and  $L_{\text{FUV}}$  (blue) in the lower panel during the pre-main-sequence evolution of a  $2 M_{\odot}$  star. The star begins with a  $0.15 M_{\odot}$  disk and an accretion rate of  $10^{-9} M_{\odot} \text{ yr}^{-1}$ . The accretion rate declines as  $t^{-3/2}$  until the effect of the FUV radiation of the star dominates. The accretion rate then stays above  $10^{-8} M_{\odot} \text{ yr}^{-1}$  for  $\sim 4$  Myr. While accretion is known to be variable and photoevaporation and planet formation may cut off accretion prior to entirely emptying the disk of gas, this scenario qualitatively captures the observed trends among IMTTs and Herbig stars.

described by P. R. T. Coelho (2014) blueward of  $2100 \text{ \AA}$  for stars ranging from 4500 to 13,000 K. The integrated flux for each time step was determined by interpolating among the measurements from the models. The effective temperature, FUV luminosity, and stellar accretion rate are then calculated for each time step. We assume that the mass of the disk is uniquely determined by the stellar accretion rate (i.e., we ignore the effects of planet formation and photoevaporation for this scenario). The stellar accretion rate, disk mass, luminosity of the FUV, and effective temperature of the star are plotted in Figure 3.

In this scenario, the disk is fully accreted after 8 Myr, and the Herbig phase ( $T_{\text{eff}} \gtrsim 7200 \text{ K}$  and  $\dot{M} \gtrsim 10^{-8} M_{\odot} \text{ yr}^{-1}$ ) lasts for 2.5 Myr. To compare the toy model with our data, we recalculated the age of our entire sample using the Siess evolutionary tracks. The uncertainty in the age was inferred from the uncertainty in the temperature and luminosity. We adopted a 0.5 dex uncertainty in the accretion rate reflecting the typical uncertainty reported in the literature. Stars with a mass within  $1\sigma$  of  $2 M_{\odot}$  were plotted, and the toy model presented in Figure 3 was plotted with the data (Figure 4).

Our toy model is only intended to capture the qualitative trend of the accretion rate as a function of age. Effects such as variable accretion, contribution to the FUV from accretion, photoevaporation, and the effect of a gap-opening planet are

not included in this model. However, the scenario we propose qualitatively matches the observed evolution of the stellar accretion rate. The youngest IMTTs are clustered near an accretion rate of  $10^{-9} M_{\odot} \text{ yr}^{-1}$ . The accretion rate of IMTTs increases as they approach the Herbig phase and maintain a relatively constant stellar accretion rate near  $10^{-7} M_{\odot} \text{ yr}^{-1}$ . This scenario also accounts for three puzzling trends observed about IMTTs and Herbig stars. First, S. L. Grant et al. (2023) note that the accretion rate of Herbig stars is relatively constant over 3 dex in disk mass. This is consistent with what we observe in Figure 3, where the stellar accretion rate hovers around  $10^{-7} M_{\odot} \text{ yr}^{-1}$  as the disk dissipates over 2.5 Myr. This stands in stark contrast to T Tauri stars, where the stellar accretion rate scales with the disk mass nearly linearly (L. Testi et al. 2022). Second, L. M. Stapper et al. (2025) compared the disk mass of IMTTs and Herbig stars. They found that the disk masses were consistent, suggesting that the accretion of disk material onto the star proceeds at a relatively slow rate during the IMTTs phase, as reflected in our model. Third, our model can account for Herbig stars with relatively low disk masses and high accretion rates.

## 5. Discussion and Conclusions

We have studied the accretion rates of intermediate-mass stars, and find that the median accretion rate of IMTTs is  $1.2 \times 10^{-8} M_{\odot} \text{ yr}^{-1}$ —more than 1 order of magnitude lower than that of their more evolved counterparts, the Herbig stars ( $1.9 \times 10^{-7} M_{\odot} \text{ yr}^{-1}$ ). The increase in the accretion rate of intermediate-mass stars as they evolve from IMTTs to Herbig stars can be explained as a consequence of the increase in their FUV luminosity.

We also showed that an increase in the accretion rate of an intermediate-mass star ( $M = 2 M_{\odot}$ ), which coincides with its pre-main-sequence temperature increase, can explain the general trends of these objects seen on the H-R diagram (Figure 2). If the stellar accretion rate scales with the FUV luminosity of the star such that the stellar accretion rate increases as the star evolves, then much lower disk masses are required to sustain the observed accretion rates among Herbig stars than if the stellar accretion rate declines with age. In the scenario we propose, a disk that begins marginally gravitationally unstable will be able to sustain an accretion rate of order  $10^{-7} M_{\odot} \text{ yr}^{-1}$  for 2.5 Myr and deplete its disk at an age of 8 Myr (near the ZAMS).

Insofar as at least some A stars accrete at significantly higher rates than their evolutionary predecessors (i.e., the IMTTs), this may motivate further investigation into the role of the FUV luminosity of the star in driving accretion. While the toy model we present does not attempt to capture the physical mechanism by which material is transported in the disk, any such model should account for the role of the FUV irradiation of the disk. Here, we discuss two other direct consequences arising from this work.

### 5.1. Weak-lined Herbig Stars

While some young intermediate-mass stars may have disk masses approaching 15% of their stellar mass, higher disk masses are unlikely. However, a few Herbig stars with accretion rates of  $10^{-7} M_{\odot} \text{ yr}^{-1}$  have ages approaching 12 Myr (Figure 4). To account for this, it is important to note that one of the original selection criteria for Herbig stars was the

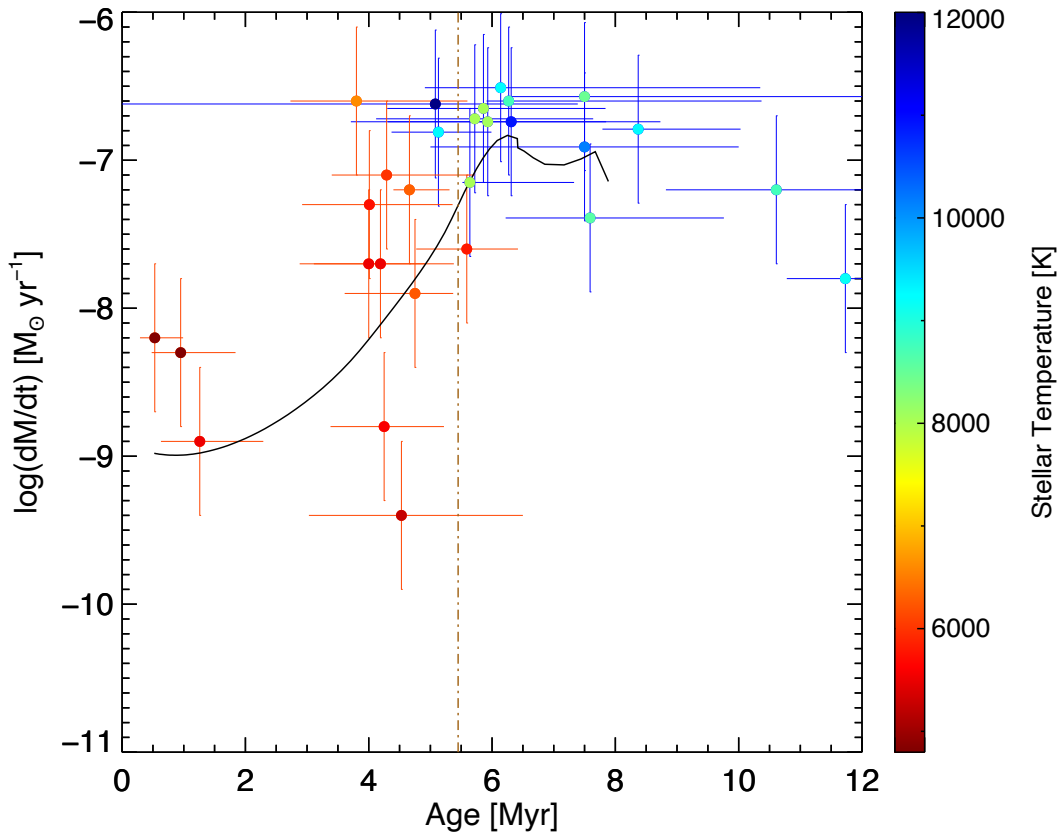


**Figure 4.** The toy model from Figure 3 is plotted against sources with masses within  $1\sigma$  of  $2 M_{\odot}$ . The IMTTs are plotted with red error bars, and the Herbig stars are plotted with blue error bars. The color of each data point corresponds to the stellar effective temperature.

association with nebulosity (G. H. Herbig 1960). There is growing evidence that such nebulae may supply additional material to disks (e.g., A. Gupta et al. 2023; J. Speedie et al. 2025, and references therein). While the replenishment of the disk from surrounding nebulae can account for the relatively long lifetime of some Herbig disks, it is not clear that this process can account for the increase in the accretion rate relative to IMTTs found here.

On the other hand, one should not expect all intermediate mass stars to have a disk mass at 0.5 Myr that is 15% of the stellar mass or that typical intermediate-mass stars accrete additional circumstellar material from surrounding nebulosity. In this case, we might expect a large population of young A stars ( $\lesssim 5$  Myr) that are the intermediate-mass analogs to weak-lined T Tauri stars (i.e., weak-lined Herbig Stars). D. P. Iglesias et al. (2023) performed a volume-limited survey ( $d < 300$  pc) of intermediate-mass stars ( $1.5 M_{\odot} \leq M_{\star} \leq 3.5 M_{\odot}$ ) with an infrared excess. They found 129 nonaccreting objects and estimate that their sample is 35%–55% complete. They classified 112 of these objects as debris disks and 17 of these objects as hybrid disks (i.e., disks in transition from protoplanetary disks to debris disks) following the classification scheme proposed by M. C. Wyatt et al. (2015). The mean age of the debris disks in their sample is 4 Myr. In the same volume and mass range, there are 30 Herbig stars, indicating that Herbig stars comprise roughly 10% of pre-main-sequence A and B stars. Thus, Herbig stars may reflect the upper end of the initial disk mass distribution captured near the end of their accretion lifetime. As noted in Section 4, S. L. Grant et al. (2023) report the short lifetimes of many disks implied by the disk masses and stellar accretion rates. These short disk lifetimes may reflect the final

stages of the transition from the Herbig phase to the “weak-lined” Herbig state.

## 5.2. Implications for Spiral Structure as a Signpost of Forming Gas Giant Planets

The results presented here also bear on the interpretation of the disk morphologies observed among Herbig stars. R. Dong et al. (2018) note the ubiquity of Herbig disks that reveal spiral structure relative to their lower mass counterparts. These authors note that this result is consistent with a higher frequency of gas giant planet formation among Herbig stars, but this result could also reflect a higher rate of disks that are not gravitationally stable. The challenge with the latter scenario is the need for long-lived massive disks, which one might naively infer from the high accretion rate of Herbig stars. However, if the scenario we propose is correct, then the stellar accretion rates measured among Herbig stars do not require the high disk masses that are 1 order of magnitude greater than the values inferred from (sub)millimeter studies (R. Dong et al. 2018). Hence, spiral structure among Herbig stars is more plausibly a signpost of gas giant planet formation. Finally, our model allows for disks with sufficient mass to form planets around Herbig stars to persist for several Myr, even at the high accretion rates observed in this evolutionary state, providing time for gas giant planet formation in these systems.

## Acknowledgments

This research has made use of the VizieR catalog access tool, CDS, Strasbourg, France (doi:10.26093/cds/vizier). The

original description of the VizieR service was published in F. Ochsenbein et al. (2000). This paper was based on Chapter 4 of the PhD thesis by J. Kern (2023).

## Appendix

Here we address two potential objections to the results presented here. One is that the stellar accretion rate of Herbig stars could be systematically overestimated. R. Dong et al. (2018) note that a large fraction of Herbig stars are  $\lambda$  Boötis stars (e.g., C. P. Folsom et al. 2012; M. Kama et al. 2015; J. Guzmán-Díaz et al. 2023) and that these stars show a UV excess in the FUV ( $\sim 1500$  Å) and near-ultraviolet ( $\sim 2300$  Å; R. O. Gray et al. 2017). One of the selection criteria for identifying  $\lambda$  Boötis candidates is based on Strömgren photometry,  $0 < \delta c_1 < 0.3$ , where  $c_1 = (u - v) - (v - b)$  is a measure of the Balmer discontinuity (E. Paunzen et al. 1997). Most studies of the stellar accretion rate of Herbig stars are based on the measurement of the Balmer discontinuity, as the accretion shock should veil this feature (J. Muzerolle et al. 2004; J. R. Fairlamb et al. 2015). The Balmer discontinuity can be measured using Johnson photometry where

$$\Delta D_B = (U - B)_0 - (U - B). \quad (\text{A1})$$

Transformation of the Johnson colors to Strömgren colors results in





$$\Delta D_B = 0.675((u - b)_0 - (u - b)) \pm 0.015, \quad (\text{A2})$$

where  $(u - b) = c_1 + 2m_1 + 2(b - y)$  (D. G. Turner 1990). To investigate the evidence for veiling of the Balmer discontinuity that could lead to a systematic overestimate of the stellar accretion rate, we calculated  $\Delta D_B$  from Strömgren photometry for 41  $\lambda$  Boötis stars compiled by E. Paunzen et al. (1997). Strömgren colors for “normal” stars were taken from G. Dalle Mese et al. (2020). We find that the  $\langle \Delta D_B \rangle$  for the sample is  $0.022 \pm 0.015$  with a standard deviation of 0.04 with a range of  $-0.06 < \Delta D_B < 0.12$ . In contrast,  $\Delta D_B$  for Herbig stars ranges from 0.05 to 1.05, with the majority of the sources ranging from 0.05 to 0.35 (J. R. Fairlamb et al. 2015). We conclude that the  $\lambda$  Boötis phenomenon is unlikely to lead to a systematic overestimate of the accretion rate of Herbig stars.

A second concern is the assumption that the magnetospheric accretion paradigm that successfully describes stellar accretion for CTTs also applies to Herbig stars. As noted above, Herbig stars do not tend to have strong, well-ordered magnetic fields, so one might expect the freefall distance to be much closer to the star or even perhaps accrete via a boundary layer. If so, then the accretion rates necessary to produce the observed UV excess would even be higher than inferred from the assumption that the stars are accreting magnetospherically (in the limit of a slowly rotating star, the accretion rate of material passing through a boundary layer would need to be twice that of material falling from infinity to produce the same accretion luminosity; D. Lynden-Bell & J. E. Pringle 1974). Furthermore, high-velocity redshifted emission is observed from these sources (M. M. Guimarães et al. 2006), which is difficult to explain via boundary layer accretion. To calculate the stellar accretion rates for this paper, we assumed that the material was falling from infinity. Given the stronger typical magnetic field strengths of IMTTs than Herbig stars, it is more likely that the stellar accretion rates of Herbig stars are underestimated relative to IMTTs. As noted in the main text,

we adopted the relationship between the luminosity of  $H\alpha$  and the accretion luminosity calibrated against T Tauri stars (J. M. Alcalá et al. 2017). Adopting the calibration for Herbig stars by J. R. Fairlamb et al. (2017) would increase the lower accretion luminosity sample by as much as a factor of 4. While the physical origin of the relationship between  $L_{H\alpha}$  and  $L_{\text{acc}}$  is not well understood, it is likely that the size of the funnel flow from the disk to the star and possibly the relationship between the accretion rate and outflow rate affect this relationship. If so, then the magnetic geometry that determines these relationships is more similar for the convective IMTTs and CTTs than it is for Herbig stars. However, calibration of the line luminosity and UV excess among IMTTs is warranted.

## ORCID iDs

Sean D. Brittain  <https://orcid.org/0000-0001-5638-1330>  
 Joshua W. Kern  <https://orcid.org/0000-0002-5860-6043>  
 Gwendolyn Meeus  <https://orcid.org/0000-0002-6251-0108>  
 René D. Oudmaijer  <https://orcid.org/0000-0001-7703-3992>

## References

- Ababakr, K. M., Oudmaijer, R. D., & Vink, J. S. 2016, *MNRAS*, **461**, 3089  
 Ababakr, K. M., Oudmaijer, R. D., & Vink, J. S. 2017, *MNRAS*, **472**, 854  
 Alcalá, J. M., Manara, C. F., Natta, A., et al. 2017, *A&A*, **600**, A20  
 Alecian, E., Wade, G. A., Catala, C., et al. 2013, *MNRAS*, **429**, 1001  
 Bai, X.-N. 2011, *ApJ*, **739**, 50  
 Bai, X.-N., & Stone, J. M. 2013, *ApJ*, **769**, 76  
 Braun, T. A. M., Yen, H.-W., Koch, P. M., et al. 2021, *ApJ*, **908**, 46  
 Brittain, S. D., Kamp, I., Meeus, G., Oudmaijer, R. D., & Waters, L. B. F. M. 2023, *SSRv*, **219**, 7  
 Calvet, N., Muzerolle, J., Briceño, C., et al. 2004, *AJ*, **128**, 1294  
 Cardelli, J. A., Clayton, G. C., & Mathis, J. S. 1989, *ApJ*, **345**, 245  
 Coelho, P. R. T. 2014, *MNRAS*, **440**, 1027  
 Dalle Mese, G., López-Cruz, O., Schuster, W. J., Chavarría-K., C., & Ibarra-Medel, H. J. 2020, *MNRAS*, **494**, 2995  
 Donehew, B., & Brittain, S. 2011, *AJ*, **141**, 46  
 Dong, R., Najita, J. R., & Brittain, S. 2018, *ApJ*, **862**, 103  
 Eisner, J. A., Hillenbrand, L. A., White, R. J., et al. 2007, *ApJ*, **669**, 1072  
 Fairlamb, J. R., Oudmaijer, R. D., Mendigutía, I., Ilee, J. D., & van den Ancker, M. E. 2015, *MNRAS*, **453**, 976  
 Fairlamb, J. R., Oudmaijer, R. D., Mendigutía, I., Ilee, J. D., & van den Ancker, M. E. 2017, *MNRAS*, **464**, 4721  
 Fang, M., Kim, J. S., van Boekel, R., et al. 2013, *ApJS*, **207**, 5  
 Flaherty, K. M., & Muzerolle, J. 2008, *AJ*, **135**, 966  
 Folsom, C. P., Bagnulo, S., Wade, G. A., et al. 2012, *MNRAS*, **422**, 2072  
 Grant, S. L., Espaillat, C. C., Brittain, S., Scott-Joseph, C., & Calvet, N. 2022, *ApJ*, **926**, 229  
 Grant, S. L., Stapper, L. M., Hogerheijde, M. R., et al. 2023, *AJ*, **166**, 147  
 Gray, R. O., Riggs, Q. S., Koen, C., et al. 2017, *AJ*, **154**, 31  
 Gregorio-Hetem, J., & Hetem, A., Jr. 2002, *MNRAS*, **336**, 197  
 Guimarães, M. M., Alencar, S. H. P., Corradi, W. J. B., & Vieira, S. L. A. 2006, *A&A*, **457**, 581  
 Gupta, A., Miotello, A., Manara, C. F., et al. 2023, *A&A*, **670**, L8  
 Guzmán-Díaz, J., Montesinos, B., Mendigutía, I., et al. 2023, *A&A*, **671**, A140  
 Hall, C., Dong, R., Rice, K., et al. 2019, *ApJ*, **871**, 228  
 Hartmann, L., Calvet, N., Gullbring, E., & D'Alessio, P. 1998, *ApJ*, **495**, 385  
 Herbig, G. H. 1960, *ApJS*, **4**, 337  
 Herbig, G. H., & Bell, K. R. 1988, Third Catalog of Emission-Line Stars of the Orion Population, Vol. 3  
 Iglesias, D. P., Panić, O., van den Ancker, M., et al. 2023, *MNRAS*, **519**, 3958  
 Janson, M., Squicciarini, V., Delorme, P., et al. 2021, *A&A*, **646**, A164  
 Jensen, E. L. N., Cohen, D. H., & Gagné, M. 2009, *ApJ*, **703**, 252  
 Johns-Krull, C. M. 2007, *ApJ*, **664**, 975  
 Kama, M., Folsom, C. P., & Pinilla, P. 2015, *A&A*, **582**, L10  
 Kern, J. 2023, PhD thesis, Clemson Univ. South Carolina <https://www.proquest.com/dissertations-theses/investigation-accretion-processes-t-tauri-herbig/docview/3059440062/se-2>  
 Kunitomo, M., Ida, S., Takeuchi, T., et al. 2021, *ApJ*, **909**, 109  
 Lynden-Bell, D., & Pringle, J. E. 1974, *MNRAS*, **168**, 603  
 Maheswar, G., Manoj, P., & Bhatt, H. C. 2003, *yCat*, J/A+A/402/963



- Manara, C. F., Testi, L., Herczeg, G. J., et al. 2017, [A&A](#), **604**, [A127](#)
- Manara, C. F., Testi, L., Natta, A., et al. 2014, [A&A](#), **568**, [A18](#)
- Mendigutía, I. 2020, [Galax](#), **8**, [39](#)
- Mendigutía, I., Calvet, N., Montesinos, B., et al. 2011, [A&A](#), **535**, [A99](#)
- Mendigutía, I., Mora, A., Montesinos, B., et al. 2012, [A&A](#), **543**, [A59](#)
- Muzerolle, J., D'Alessio, P., Calvet, N., & Hartmann, L. 2004, [ApJ](#), **617**, [406](#)
- Najita, J. R., Andrews, S. M., & Muzerolle, J. 2015, [MNRAS](#), **450**, [3559](#)
- Natta, A., Testi, L., & Randich, S. 2006, [A&A](#), **452**, [245](#)
- Ochsenbein, F., Bauer, P., & Marcout, J. 2000, [A&AS](#), **143**, [23](#)
- Paunzen, E., Weiss, W. W., Heiter, U., & North, P. 1997, [A&AS](#), **123**, [93](#)
- Perez-Becker, D., & Chiang, E. 2011, [ApJ](#), **735**, [8](#)
- Reipurth, B., Pedrosa, A., & Lago, M. T. V. T. 1996, [A&AS](#), **120**, [229](#)
- Rojas, G., Gregorio-Hetem, J., & Hetem, A. 2008, [MNRAS](#), **387**, [1335](#)
- Sicilia-Aguilar, A., Hartmann, L. W., Fűrész, G., et al. 2006, [AJ](#), **132**, [2135](#)
- Siess, L., Dufour, E., & Forestini, M. 2000, [A&A](#), **358**, [593](#)
- Simon, M. N., Pascucci, I., Edwards, S., et al. 2016, [ApJ](#), **831**, [169](#)
- Speedie, J., Dong, R., Teague, R., et al. 2025, [ApJL](#), **981**, [L30](#)
- Stapper, L. M., Hogerheijde, M. R., van Dishoeck, E. F., & Mentel, R. 2022, [A&A](#), **658**, [A112](#)
- Stapper, L. M., Hogerheijde, M. R., van Dishoeck, E. F., et al. 2025, [A&A](#), **693**, [A286](#)
- Testi, L., Natta, A., Manara, C. F., et al. 2022, [A&A](#), **663**, [A98](#)
- Turner, D. G. 1990, [PASP](#), **102**, [1331](#)
- Valegård, P. G., Waters, L. B. F. M., & Dominik, C. 2021, [A&A](#), **652**, [A133](#)
- Villebrun, F., Alecian, E., Hussain, G., et al. 2019, [A&A](#), **622**, [A72](#)
- Vink, J. S. 2015, [Ap&SS](#), **357**, [98](#)
- Vink, J. S., Drew, J. E., Harries, T. J., & Oudmaijer, R. D. 2002, [MNRAS](#), **337**, [356](#)
- Vink, J. S., Drew, J. E., Harries, T. J., Oudmaijer, R. D., & Unruh, Y. 2005a, [MNRAS](#), **359**, [1049](#)
- Vink, J. S., Harries, T. J., & Drew, J. E. 2005b, [A&A](#), **430**, [213](#)
- Vioque, M., Oudmaijer, R. D., Baines, D., Mendigutía, I., & Pérez-Martínez, R. 2018, [A&A](#), **620**, [A128](#)
- Walter, F. M. 1992, [AJ](#), **104**, [758](#)
- Wichittanakom, C., Oudmaijer, R. D., Fairlamb, J. R., et al. 2020, [MNRAS](#), **493**, [234](#)
- Wyatt, M. C., Panić, O., Kennedy, G. M., & Matrà, L. 2015, [Ap&SS](#), **357**, [103](#)